

GPR Characteristics of Ore-Bearing Layered Igneous Bodies

Nigel J. Cassidy

Applied and Environmental Geophysics Group, School of Physical Sciences & Geography, Keele University,
Keele, Staffordshire, ST5 5BG, UK.

n.j.cassidy@esci.keele.ac.uk

ABSTRACT

For many geological materials, the magnetic properties of the constituent parts are often considered unimportant when compared to their 'dielectric' characteristics (i.e., the permittivity and conductivity). However, if significant amounts of iron sulphide and/or magnetic minerals exist (such as magnetite, pyrrhotite, etc) then the EM relaxation phenomena of these minerals can have a noticeable effect on the GPR wave's attenuation and propagation velocity. Both surface and borehole-based GPRs have been successfully used to delineate and map layered igneous ore bodies but subtle, natural, variations in magnetite/ore mineral composition, grain size and mineral fabric can all have an effect on the nature of the GPR responses. In this paper, we present the latest findings of a measurement and analysis study on the GPR-related apparent permittivity, attenuation and propagation velocity characteristics of a range of natural occurring, magnetite/ore-rich igneous samples collected from the Bushveld complex, South Africa.

Key words: Ground penetrating radar, dielectric analysis, ore body materials, Bushveld.

INTRODUCTION

Ground-penetrating radar (GPR) is, arguably, the most popular, broad-based geophysical technique for near-surface ground investigation due to its unrivalled ability to stratigraphically map large areas of ground in relatively short times. Unfortunately, the processing and interpretation of GPR data can be both difficult and time consuming, particularly in complex, heterogeneous environments. In the past few years, advanced modelling and interpretation methods (such as finite-difference time domain modelling and tomographic inversion techniques) have lead to more sophisticated data analysis approaches and the ability to 'extract' material property information from the GPR data (e.g., Cassidy and Millington, 2009). This degree of interpretational refinement has allowed GPR to significantly expand its use in application areas such as land contamination, hydrology and, more specifically, ore-related mining. In part, this development is due to advances in GPR system design (including directional borehole GPR, multi-antenna array systems, etc) but also to our improved ability to relate GPR signal responses to the actual electromagnetic properties of the host materials.

Borehole-based GPR investigation methods have been used to successfully map igneous bodies (Simmat et al., 2006; Van Schoor et al., 2006; Du Pisani and Vogt, 2004) but there has been limited published information on the effect of natural, crystalline, magnetite/ore-rich

materials on the GPR signal's attenuation/propagation characteristics. For many igneous rocks, the variation in electromagnetic (EM) properties can be subtle with little variation between geologically dissimilar materials. However, if significant amounts of magnetic minerals exist (e.g., magnetite, maghemite, etc.) and/or disseminated iron sulphide phases are present (such as pentlandite, pyrrhotite and chalcopyrite) then the magnetic/dielectric relaxation phenomena of these minerals can have a significant effect on the complex apparent permittivity spectrum of the material as a whole (Cassidy, 2008). As a consequence, the GPR wave attenuation and propagation velocities of the bulk materials can vary significantly over relatively small spatial scales (metres or less). Recent studies on fine-scaled, magnetite-rich mixtures in particular (both natural and simulated) have shown that the magnetically lossy materials can have a significant influence on the measured complex apparent permittivity, velocity and attenuation with increasing permittivities (both real and imaginary components) being observed with increasing magnetite content (Cassidy, 2008; Thomas et al., 2008). However, there is still some doubt to the extent of this effect in natural, crystalline magnetite ore rocks, particularly where changes in grain size, composition, spatial distribution or layered fabric occur within the rocks. In order to provide a degree of quantitative control on these factors, we present the latest findings of a laboratory-based investigation into the GPR-related apparent permittivity, velocity and attenuation

properties of these natural magnetite/ore-rich igneous material collected from the across the Bushveld Igneous Complex, South Africa.

APPARENT PERMITTIVITY MEASUREMENTS

The apparent permittivity of a range of Bushveld samples (including Norites, Mottled Anorthosites Titaniferous Magnetite, Magnetite Gabbros, Pyroxenites and Chromitites – including Merenskey reef samples) were evaluated in the laboratory using a dielectric analysis technique incorporating an Agilent Technologies 8753ES Automated Vector Network Analyser (or ANA), calibrated reflection test probe set and an automated measurement/inversion technique that converts the measured S-parameters into a complex apparent permittivity spectrum. The method is well established and has been used to measure a wide range of sub-surface materials including soils and rocks (Baker-Jarvis, 1990; Bryant, 1988). The measurement process produces a frequency-dependent, complex apparent permittivity that includes all the loss effects associated with the analysed material, regardless of the physical attenuation mechanisms (e.g., dipolar/lattice dislocation permittivity losses and/or magnetic moment spin and domain wall interaction losses). The results can then be used directly with the conventional GPR attenuation and velocity equations (in the form of 1 & 2 below) allowing the electromagnetic behaviour of the materials to be described in a generic form without having to attribute the loss and propagation effects to any specific ‘electric’ or ‘magnetic’ phenomenon.

$$\alpha(\omega) = 8.686\omega \sqrt{\left[\frac{\mu(\omega)\epsilon'(\omega)}{2} \sqrt{1 + \tan^2 \delta(\omega)} - 1 \right]} \quad (1)$$

$$v(\omega) = c \left(\sqrt{\left[\frac{\epsilon'(\omega)}{2\epsilon_0} \sqrt{1 + \tan^2 \delta(\omega)} + 1 \right]} \right)^{-1} \quad (2)$$

- α frequency-dependent attenuation co-efficient in dBm^{-1} .
- v frequency-dependent phase velocity in ms^{-1} .
- μ free-space magnetic permeability (in Hm^{-1}).
- ϵ' real component of the frequency-dependent apparent permittivity (in Fm^{-1}).
- ϵ'' imaginary component of the frequency-dependent apparent permittivity (in Fm^{-1}).
- ϵ_0 permittivity of free space (in Fm^{-1}), real valued and constant.
- w angular frequency (in Radians/s) given by $w = 2\pi f$ where f is the GPR signal frequency in Hz.
- c velocity of EM waves in free space.
- $\tan \delta$ loss tangent (or loss factor) of the material and is determined from $\epsilon''(\omega)/\epsilon'(\omega)$.

In order to obtain the most appropriate value of apparent permittivity for each sample, multiple measurements were made at different positions on a polished face. The full set of results were then averaged to produce a mean value of apparent permittivity for each sample with error limits set to one standard deviation from the mean (typically less than 5% error).

APPARENT PERMITTIVITY RESULTS

Figures 1-3 illustrate the complex, apparent relative permittivity measurements (including errors) plus the signal attenuation and velocity characteristics for a number of representative ‘magnetite-rich’ Bushveld samples including :

Magnetite Gabbro Ore	(~68% Magnetite, BS 51c)
Magnetite Gabbro	(~23% Magnetite, BS 1a)
Titaniferous Magnetite	(~96% Magnetite, BS 40)
Norite	(~7% Magnetite, BS 46)

The measured apparent permittivities of these samples clearly illustrate the differences in their EM characteristics across the common GPR frequency range (10-1500MHz).

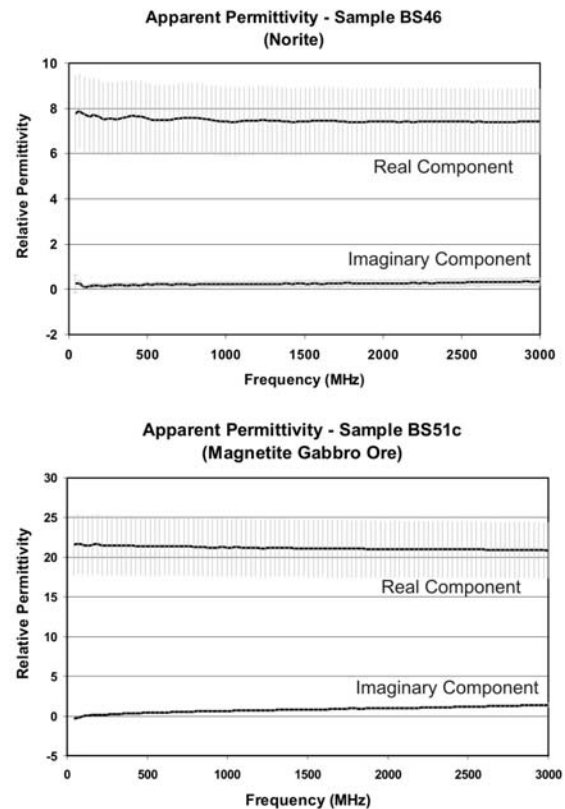


Figure 1. Complex apparent permittivity of samples BS 46 (Norite) and BS 51c (Magnetite Gabbro Ore).

As would be expected, the low-percentage magnetite Norite (BS 46) and Magnetite Gabbro samples have almost constant, low values of apparent permittivity for the real component (~7.7 and 9 respectively) whilst the magnetite-rich samples (BS 51c, Magnetite Ore and BS

40, Titaniferous Magnetite Ore) have relatively high apparent permittivity values of about ~18-20.

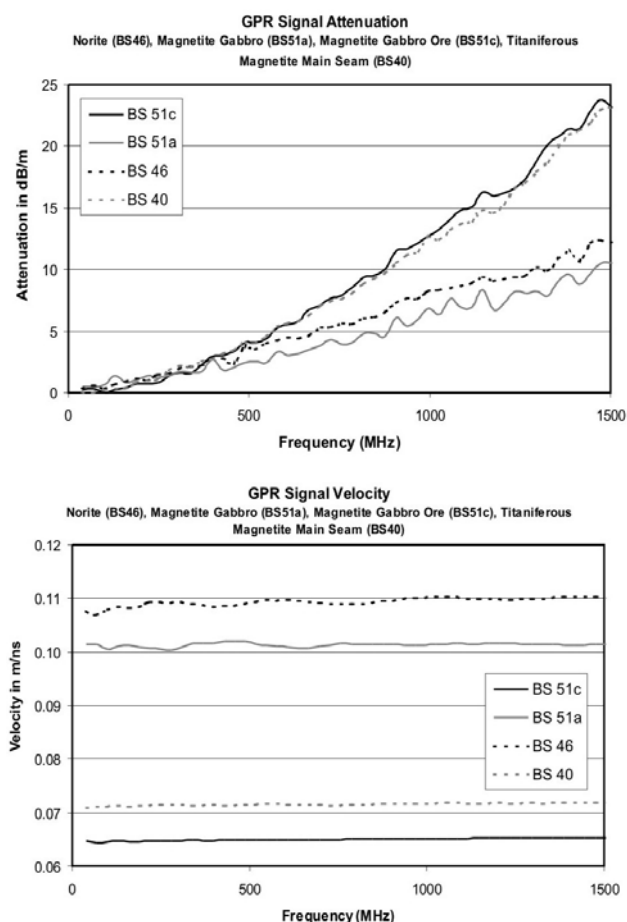


Figure 2. Attenuation and velocity characteristics over the common GPR frequency range of 40MHz – 1500MHz for the (Norite), BS 51a (Magnetite Gabbro), BS 51c (Magnetite Gabbro Ore) and BS 40 (Titaniferous Magnetite Ore) samples. Note : error bars have been omitted for visual clarity.

All samples tend to show slightly increasing trends for the imaginary component of the apparent permittivity but with comparable values (i.e., all values are less than 2). This is consistent with low-loss materials that do not exhibit any significant magnetic relaxations in the measured GPR frequency range.

The Norite and Magnetite Gabbro rocks show appreciably different velocity values to the Magnetite Ore samples that would result in high GPR signal reflectivities at any sharp interface boundaries. With a reflection coefficient value, R , of about 0.2, this would be consistent with other ‘high-contrast’ features such as dry/saturated soils ($R \sim 0.3$) and rock/soil ($R \sim 0.15$) and produce signal responses that could be easily identified in any GPR section. More importantly, it would mean that significant signal scattering would occur if the form of the interface varied at sub-wavelength scales, either as ‘topographic’ undulations or disaggregated, mixed-flow units.

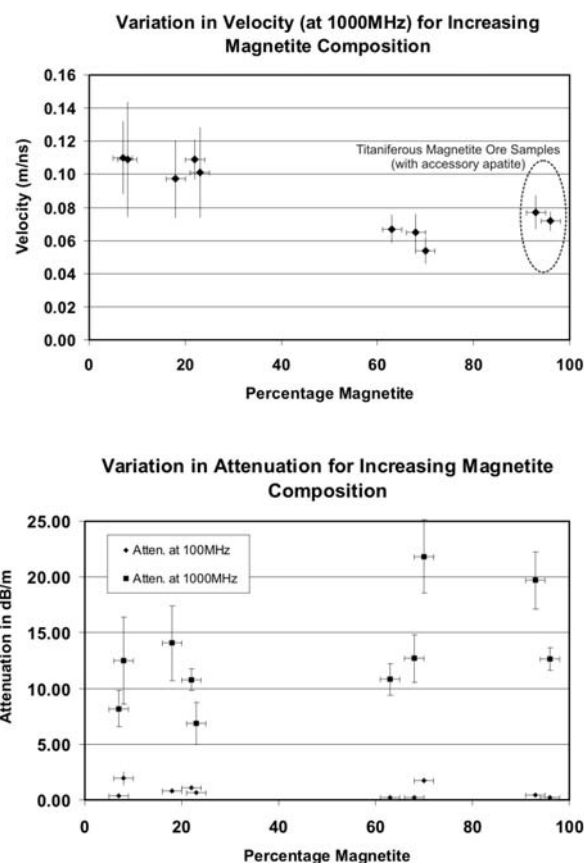


Figure 3. Variation in GPR signal attenuation and velocity with increasing percentage magnetite content for all samples at 1000MHz (velocity and attenuation) and 100MHz (attenuation).

The velocity characteristics of the Norite and Gabbro samples appear to follow a simple trend with decreasing velocity relating to increasing magnetite content (figure 3). Although shown at a frequency of 1000MHz, the results are almost identical across the whole GPR frequency range indicating that the velocity response is frequency-independent and, therefore, propagation will non-dispersive. With the Titaniferous Magnetite Ore samples (>90% Magnetite), the velocity increases away from the linear trend with values that are approximately 30% faster. This is most likely due to significant amounts of ‘non-magnetic’ apatite being included in the bulk magnetite percentage during petrological analysis.

The equivalent attenuation characteristics are particularly interesting as it would seem that at low frequencies (<100MHz), all the rocks are effectively low-loss with material attenuations of less than ~2dB/m (figure 3). The attenuation only becomes important at higher frequencies (10-25dB/m at 1000MHz) with a slight increase in attenuation associated with increasing magnetite content.

Figure 4 illustrates how the apparent permittivity measurements can also be used in a more practical way to produce ‘virtual logs’ of frequency-averaged GPR

signal velocity and attenuation. The example shown is a 'log' taken through a concordant sequence in the main Bushveld economic zone and includes Anorthosites (POIKAN), Norites (N), Pyroxenites (PYX), Pegmatoidal Pyroxenite (PEGFPPYX) and ore-bearing Chromites (CR) as thin, centimetre-thick bands/stringers.

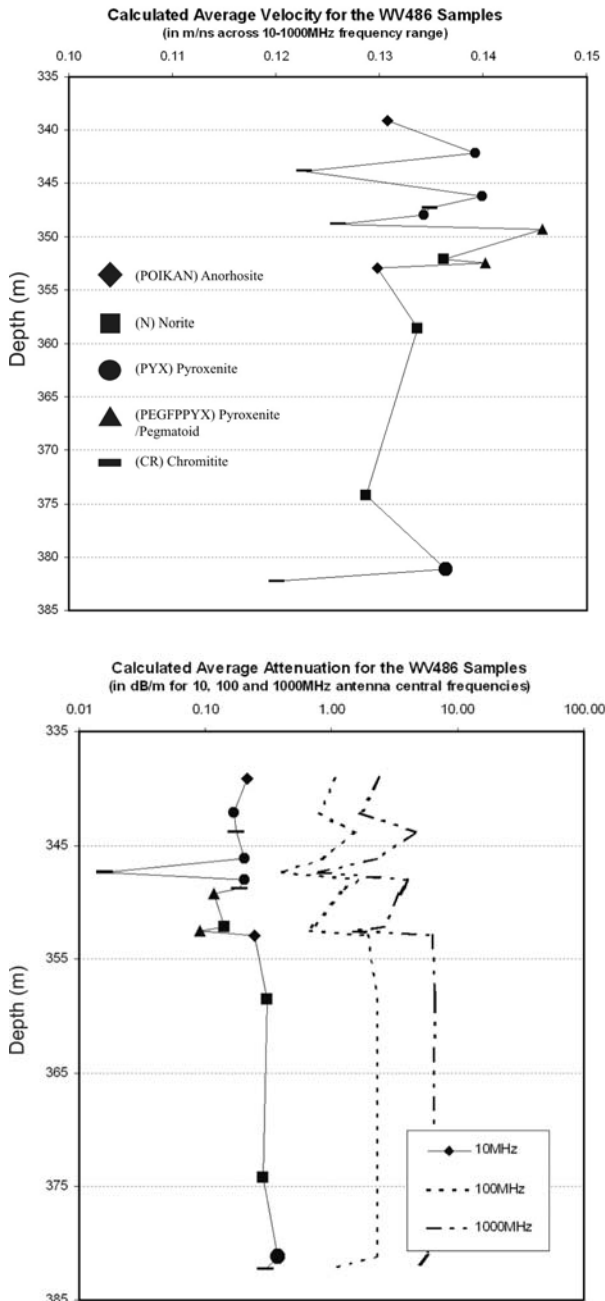


Figure 4. Frequency-averaged (10-1000MHz) GPR signal velocity and attenuation 'log' for a concordant sequence of the Bushveld ore-bearing rocks.

As with the magnetite-rich samples, the results show significant velocity variation between individual units (particularly the chromites) resulting in contrasting, reflection interfaces being present in the sequence. The strongest of these will be associated with the individual

ore-bearing, economic, seams (e.g., the chromite-pyroxenite boundaries between 344-350m) but other non-economic interfaces (i.e., the Anorthosite-Pegmatoidal Pyroxenite contact at 352m) may also provide enough of a material property contrast to generate complex reflection responses in this important zone. In contrast, the attenuation 'log' shows little variation between the samples at lower frequencies (i.e., 0.1 – 0.5 db/m at 10MHz and 0.5 – 3 db/m at 100MHz), with the exception of a single chromitite sample at ~348m. Even at the highest frequencies, material attenuation levels are below ~8db/m, which is consistent with the low-loss characteristics of the magnetite/ore-rich samples in the previous figures.

CONCLUSIONS

The results of this on-going study into the GPR-related dielectric, velocity and attenuation properties of magnetite/ore-rich materials show that even relatively low amounts of magnetite (or iron sulphides as inclusions in the ore-bearing chromitite seams) can have a considerable effect on GPR wave propagation and velocity, but not attenuation. As such, GPR signal velocity and reflection amplitude could be used as a proxy tool for deposit mapping, mineral phase characterisation and, potentially, for obtaining composition percentages directly from the GPR data.

ACKNOWLEDGMENTS

The authors would like to thank Peter Greatbatch and David Wilde for preparing the samples and Dr Petro du Pisanin . The research has been funded, in part, by NERC grant NER/2002/00100, EPSRC grant EP/004032/1 (IMAGINE project - Inversion, Modelling and Analysis of GPR in Near-Surface Environments) and a Royal Society Industrial Fellowship awarded to the author.

REFERENCES

- Baker-Jarvis J., 1990. Transmission/Reflection and Short-Circuit Line Permittivity Measurements, United States Department of Commerce, National Institute of Standards and Technology, NIST Technical Note 1341, Boulder Colorado, USA (1990).
- Bryant G. H., 1988. Principles of Microwave Measurement, IEE Electrical Measurement Series 5, Peter Peregrinus Ltd. London, U.K.
- Cassidy, N. J., 2008. GPR Frequency-Dependent Attenuation and Velocity Characteristics of Nano-to-Micro Scale, Lossy, Magnetite-Rich Materials, Near Surface Geophysics, 6, 6, 341-355.
- Cassidy, N. J. and Millington, T. M., 2009. The Application of Finite-Difference Time-Domain Modelling for the Assessment of GPR in Magnetically Lossy Materials. Journal of Applied Geophysics, 67, 4, 296-308.

Du Pisani, P. and Vogt, D., 2004. Borehole radar delineation of the Ventersdorp Contact Reef in three dimensions, *Exploration Geophysics*, 35, 319–324.

Simmat, C. M. P., Herselman, P. R., Rutschlin M., I. Mason M. and Cloete J. H., 2006. Remotely sensing the thickness of the Bushveld Complex UG2 platinum reef using borehole radar, *Journal of Geophysics and Engineering*, 3, 43–49.

Thomas, A. M., Burrow, M. P. N., Rogers, C. D. F., Chapman, D. N., Metje, N., Dunn G. and Nelder, L., 2008. Electromagnetic Characterisation of a Victorian Railway

Embankment Fill Material, Proceedings of the 3rd International Conference on Site Characterization 2008, Taipei, Taiwan, 1-6.

Van Schoor M., Du Pisani P. and Vogt D., 2006. High-resolution, short-range, in-mine geophysical techniques for the delineation of South African orebodies, *South African Journal of Science*, 102, 355-360.